JOURNAL OF MATERIALS SCIENCE 11 (1976) 1600–1606

Quantitative aspects of precipitation at grain boundaries in an austenitic stainless steel

A. R. JONES, P. R. HOWELL, B. RALPH
Department of Metallurgy and Materials Science, University of Cambridge, UK

This paper shows, in a quantitative manner, how the precipitation of niobium carbide in an austenitic stainless steel is affected by varying the amount of deformation prior to ageing. In particular, the extrinsic dislocation content of grain boundaries is shown to govern the overall size distribution of grain-boundary precipitates developed during ageing.

1. Introduction

In a previous paper it was shown that non-equilibrium grain-boundary defect structures played an important role in determining the heterogeneous nucleation behaviour of a second phase (niobium carbide (NbC)) at the grain boundaries in an austenitic stainless steel [1]. The present investigation, which is an extension of the above mentioned work, has concentrated on establishing quantitative aspects of the size distribution of particles at grain boundaries. During this investigation, quantitative data were also obtained from other microstructural regions of the specimens studied.

An overall comparison of the quantitative data obtained, shows that particle size distributions established during ageing are a sensitive function of the degree of prior deformation.

2. Experimental details

The alloy investigated had a composition of 20 wt% chromium, 25 wt% nickel, 0.5 wt% niobium 0.05 wt% carbon + nitrogen, balance iron.

Three different thermomechanical treatments were studied: (a) solution treated at 1350° C, quenched, 10% cold-rolled and aged for $\frac{1}{2}$h at 930° C; (b) as for (a) except with only a 5% cold-roll prior to ageing; (c) as for (a) but with no deformation prior to ageing.

The above percentages of cold-rolling are defined as reductions in specimen thickness.

Both qualitative and quantitative data on the above specimen states were obtained using electron microscopy. Thin foil specimens were used to provide qualitative data, while carbon extraction replicas were used in the acquisition of quantitative particle size distribution data. The microscope used in the investigation was a Philips EM 301. Quantitative data were obtained from the carbon extraction replicas using a Quantimet 720 image analysing computer equipped with full pattern recognition facilities. Further details of the methods of data acquisition and data analysis may be found elsewhere [2, 3].

3. General observations from carbon extraction replicas

Fig. 1a to c show typical areas of carbon extraction replicas obtained from specimens of the 0%, 5% and 10% deformed and aged specimens, respectively. During a preliminary stage of the investigation, it became apparent from the observation of carbon extraction replicas that, although for all three specimen states there were two distinct and easily identifiable microstructural regions, for the deformed specimens a third microstructural region existed. For all three specimen states, matrix and grain-boundary regions were clearly apparent. However, in the replicas obtained from specimens which had been deformed prior to ageing, a third, less obvious microstructural region was apparent; this was the precipitate-depleted zone close to each grain boundary. The population density and size distributions of precipitates in these latter regions were affected by the presence of each

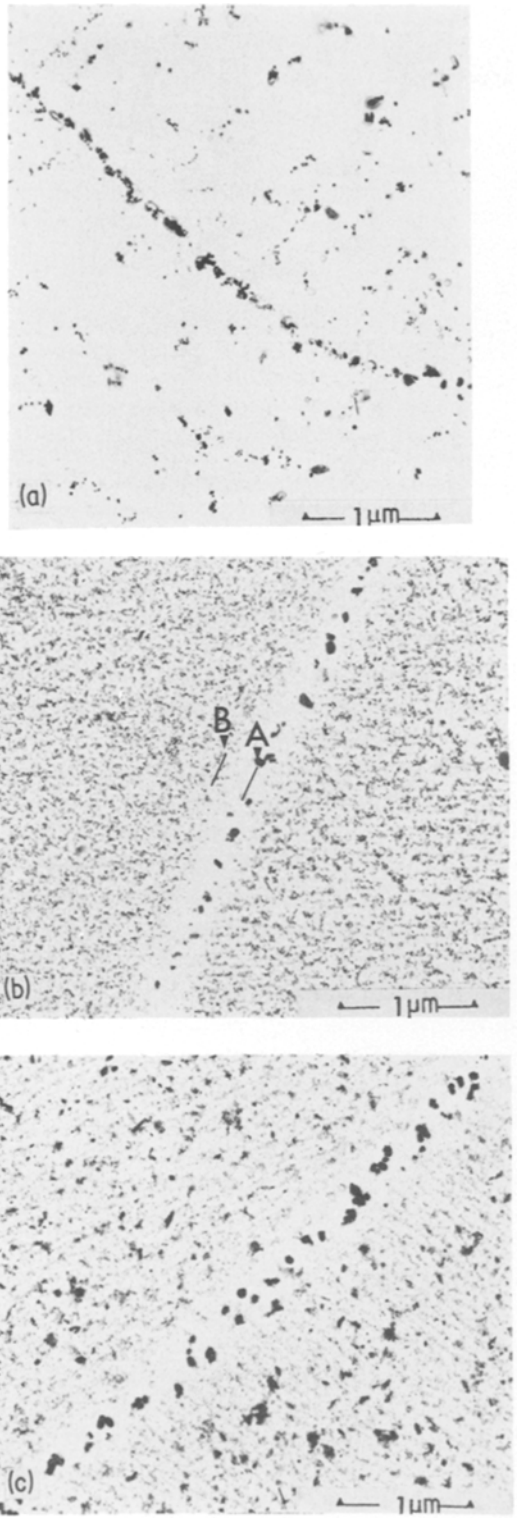

Figure 1 Carbon extraction replicas showing precipitates in a specimen which (a) had received no deformation prior to ageing. (b) was deformed by 5% prior to ageing (see text) and (c) had been deformed by 10% prior to ageing.

neighbouring grain boundary.

General observations of the carbon extraction replicas did establish that there were marked variations in the size distributions of NbC particles from grain boundary to grain boundary in specimens of the same thermomechanical state. Such variations are established in a quantitative manner in the following sections, while comparisons are also made between identical microstructural regions from different specimen states. Although the quantitative data concerning the size distribution of particles in the precipitate depleted zones are less accurate and less significant than those concerning the other microstructural regions, the importance of the presence of such precipitate depleted zones is considered in greater detail in later sections.

Further, general observations from the examination of carbon extraction replicas indicated that the number density of NbC precipitates was a sensitive function of both the microstructural region analysed and the thermomechanical history of the specimen examined. Hence, the number density of grain boundary and matrix precipitates tends to increase as the level of deformation increases (and see Sections 4 and 5).

4. The quantitative analysis of particle size distribution data

4.1. The matrix regions

Quantitative data, averaged over the matrix regions of specimens of all three of the thermomechanical treatments, showed a consistent trend relating the mean particle size measured to the degree of deformation introduced prior to ageing. With increasing amounts of deformation, the measured mean size of the matrix particles decreased. Such a correlation is perhaps not unexpected, since increasing the level of deformation increases the number of potential heterogeneous nucleation sites present in the matrix. A qualitative impression of the differences in nucleation density in the matrix of specimens of different deformation levels may be obtained by examining the matrix regions shown in Fig. 1a and b; the density of precipitation being much higher in the deformed specimen. Hence, overall size differences in the matrix from specimen state to specimen state are a reflection of nucleation density and the smaller extent of the diffusion fields associated with individual particles in the more heavily deformed specimens.

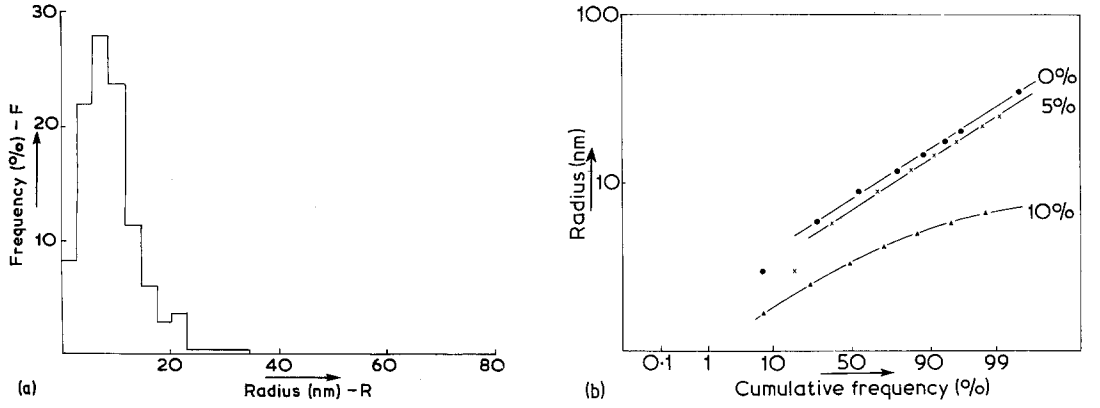

Figure 2(a) The relative volume frequency/size distribution plot of matrix particle sizes averaged over all data obtained from specimens which were undeformed prior to ageing. (b) Log-normal/probability plots showing the data contained in (a), together with particle size information averaged over all matrix regions of specimens deformed by 5% and 10% prior to ageing.

Fig. 2a shows a relative volume frequency/size distribution plot averaged over all of the matrix regions measured in specimens which were undeformed prior to ageing. A log-normal/probability plot of the data assembled in the form of a cumulative frequency is shown together with similar data from the 5% and 10% cold-worked specimen states in Fig. 2b. The plots from the specimens deformed by 0% and 5% prior to ageing can be seen to be very close to log-normal in nature. The plot of the data obtained from the specimens deformed by 10% prior to ageing can be seen to be slightly skew log-normal in nature.

The actual mean radial size of the NbC particles, calculated for the matrix regions of the three specimen states analysed, were 3.5 nm for the 10% deformed specimens, 7.5 nm for the 5% deformed specimens and 9.3 nm for the undeformed specimens.*

4.2. The grain boundaries

Fig. 3a to d show relative volume frequency/size distribution plots obtained from four different grain boundaries in specimens deformed by 5% prior to ageing. These plots confirm the observations noted in Section 3 that particle sizes vary markedly from grain boundary to grain boundary in specimens of the same thermomechanical history. The measured mean particle sizes can be seen to vary between 8.5 and 29 nm. Log-normal/probability plots of the data contained in these figures are shown in Fig. 3e. Although the plots are non-linear in nature, the shape of the distributions appear to be more closely represented by skew log-normal plots rather than by any of the other standard shapes of probability curves (e.g. a simple normal distribution).

Similar variations in mean particle size from grain boundary to grain boundary were found in the other specimen states analysed. However, when the overall mean particle size for the grain-boundary regions of each specimen state were calculated and compared a consistent change was found, whereby this mean size increased with increasing cold-work prior to ageing. This is the converse of the situation pertaining to the matrix regions where the mean matrix particle size was found to decrease with increasing levels of cold-work prior to ageing. For the specimens which had received no cold-work prior to ageing the mean grain-boundary particle size was found to be 14 nm, while for the specimens deformed by 5% and 10% prior to ageing the mean grain-boundary particle sizes were 17.5 and 19 nm respectively.

The reasons for the occurrence of the above noted divergence between the mean particle sizes in the matrix and the mean particle sizes in the grain boundaries as the level of deformation introduced prior to ageing is increased will be discussed in Section 5.

* Although the quoted values for mean sizes imply an accuracy and resolution well in excess of that actually obtained, they are in fact convenience measurements which result from the stereological modelling process used in their final estimation (namely the equivalent circle measurement of e.g. [4] and see [2]).

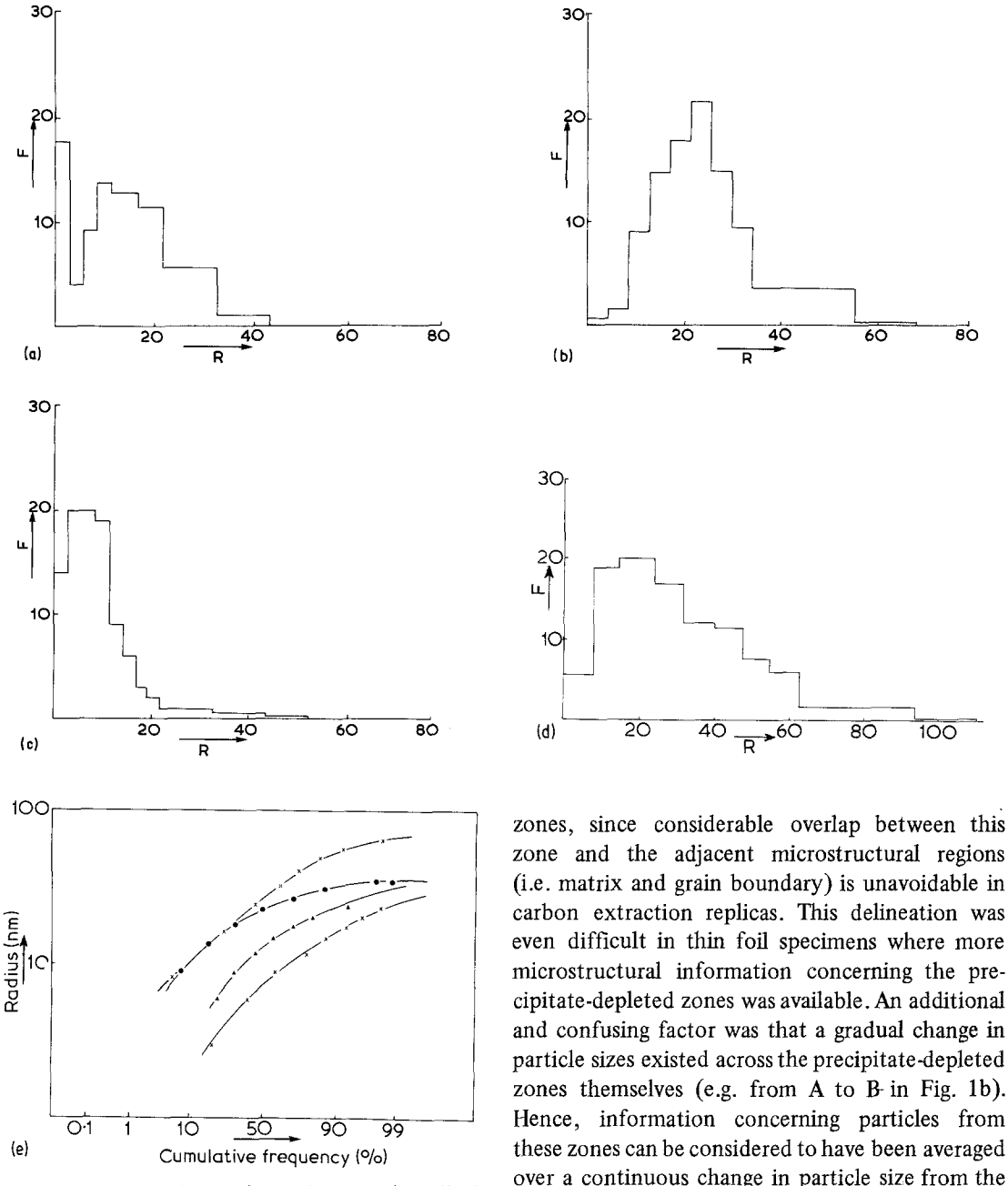

Figure 3(a) to (d) Relative volume frequency/size distribution plots from four different grain boundaries in specimens deformed by 5% prior to ageing. (e) Log-normal/probability plots of the data contained in (a) to (d).

4.3. Precipitate depleted zones

As noted in Section 3, precipitate-depleted zones were seen to be associated with most grain boundaries in specimens which had been deformed prior to ageing. It was difficult to make accurate quantitative measurements of the mean size of particles present in the precipitate-depleted zones, since considerable overlap between this zone and the adjacent microstructural regions (i.e. matrix and grain boundary) is unavoidable in carbon extraction replicas. This delineation was even difficult in thin foil specimens where more microstructural information concerning the precipitate-depleted zones was available. An additional and confusing factor was that a gradual change in particle sizes existed across the precipitate-depleted zones themselves (e.g. from A to B in Fig. 1b). Hence, information concerning particles from these zones can be considered to have been averaged over a continuous change in particle size from the boundary to the unaffected matrix regions.

The mean radial size of the particles measured in the precipitate depleted zones in both the 5% and the 10% deformed specimens was found to be less than 1.5 nm. A typical size distribution for a precipitate depleted zone in a specimen deformed by 5% prior to ageing is shown in Fig. 4. Similarly, the peak that is seen at small particle sizes in Fig. 3a is, in fact, due to the unavoidable collation of particles from the precipitate depleted zone with those from the grain boundary region.

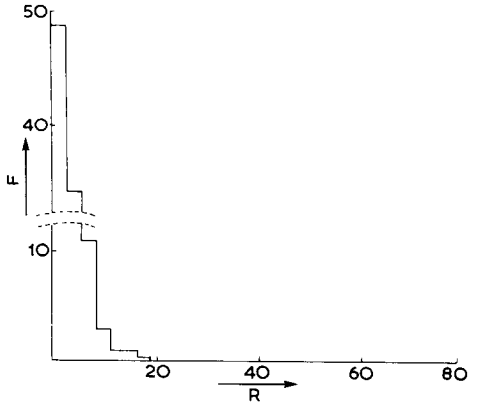

Figure 4 A typical relative volume frequency/radial size distribution plot from a precipitate depleted zone. The specimen was deformed by 5% prior to ageing.

5. Correlation between deformation and precipitation behaviour

The results noted in Section 4 related the size distributions of NbC precipitates to the level of prior deformation. This section will correlate these observations with the total microstructures developed during the thermomechanical processing of the specimen materials, as observed using transmission electron microscopy of thin foils.

5.1. Matrix precipitation

The size distributions collated from the matrix regions showed that the mean carbide size decreased as the level of deformation increased. This may be explained in terms of the heterogeneous nucleation and growth behaviour of the precipitates (e.g. Section 4.1). Fig. 5a and b show typical examples of thin foil observations of the matrix microstructure away from the grain boundaries in two different specimen states. In both cases, the NbC precipitates can be seen to be associated with the dislocation substructures that are present.

5.2. Grain-boundary precipitation and the precipitate depleted zones

5.2.1. The precipitate distributions

The results obtained from the quantitative analysis of the grain-boundary regions can be summarized as follows:

(1) for any one thermomechanical state, the mean carbide size varies considerably from boundary to boundary;

(2) the mean carbide size at the boundaries increases as the level of deformation increases (see Section 4.2);

(3) precipitate-depleted zones were associated with boundaries in specimen material which had been deformed prior to ageing;

(4) the number density and mean size of the precipitates in the depleted zones was significantly lower than that found in the abutting matrix regions.

5.2.2. The dislocation distributions

Deformation of the specimen material leads to the production of matrix dislocations and grain-boundary extrinsic dislocations. During any subsequent annealing process (e.g. the early stages of ageing), thermally induced interaction between matrix dislocations and the grain boundary will allow certain of the matrix dislocations to glide into the boundary where they will form extrinsic dislocations. As a consequence of this process, a

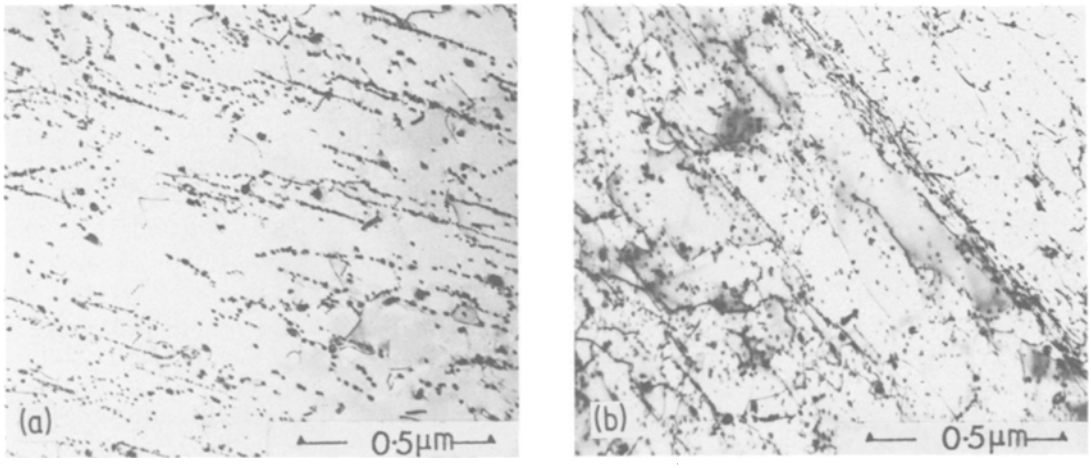

Figure 5 Thin foil observations of typical regions of the matrix in specimens which had received (a) 5% deformation prior to ageing, (b) 10% deformation prior to ageing.

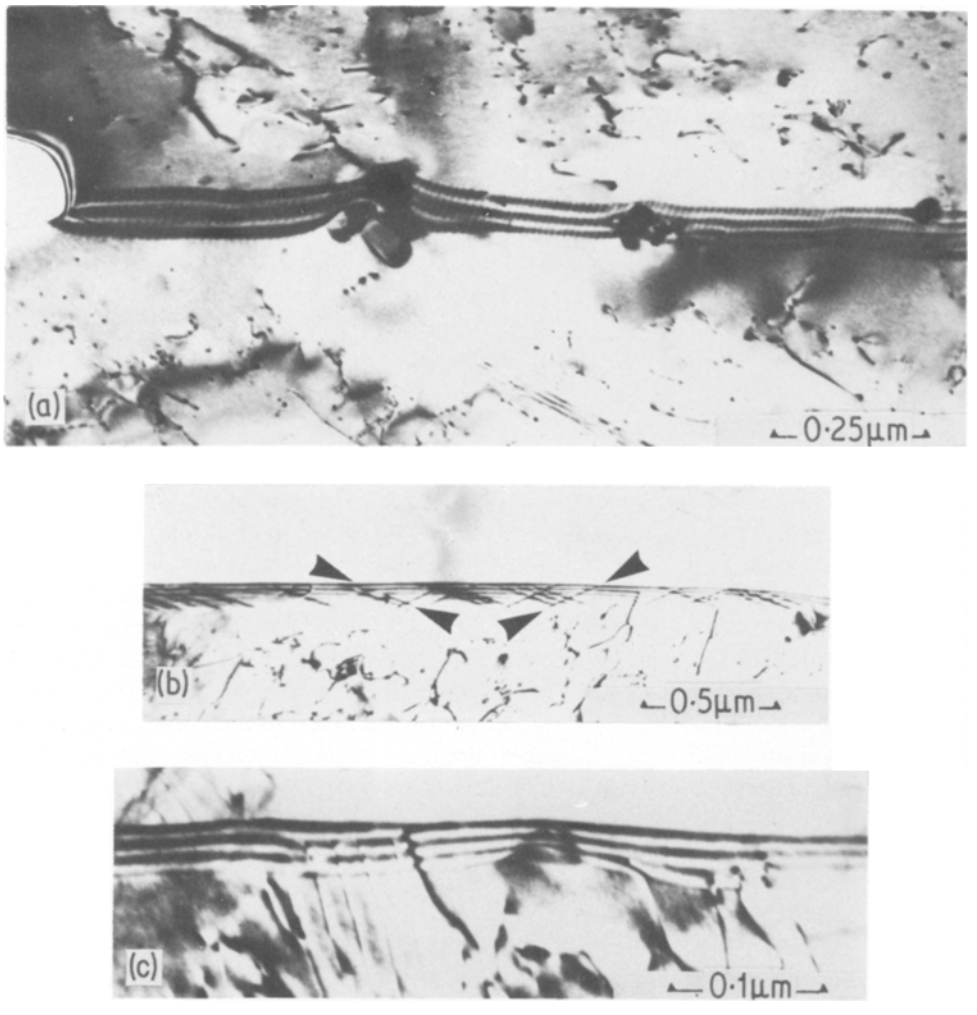

Figure 6(a) Dislocation and precipitate-depleted zones close to a grain boundary in a specimen deformed by 10% prior to ageing. (b) A grain boundary containing two sets of extrinsic dislocations (arrowed) in a deformed and aged specimen. (c) "Dislocation links" between a grain boundary and an abutting matrix region in a 10% deformed and aged specimen.

dislocation depeleted zone will be created adjacent to the boundary. The types of microstructure produced by these processes are shown in Fig. 6a to c. In Fig. 6a the reduction in matrix dislocation density close to a grain boundary is illustrated. It should be noted that an attendant depletion of precipitate number density accompanies this dislocation depletion. In Fig. 6b, two extrinsic dislocation arrays are observed (arrowed) whilst in Fig. 6c, dislocations are observed which are partially contained in the boundary (extrinsic) and partially in the abutting grain (matrix), leading to the formation of "dislocation links" between matrix and boundary. The number density of extrinsic dislocations was found to be higher in the specimens which had received 10% cold-work prior to ageing than in specimens which had received 5% deformation prior to ageing. Similarly the presence of "dislocation links" and the observation of more than one set of extrinsic dislocations, in the grain boundaries of the specimens analysed, was more frequent in specimens which had been deformed by 10% prior to ageing than in specimens which had received 5% deformation prior to ageing. The above microstructural features were rarely seen in specimens which had not been deformed prior to ageing.

In summary, the deformation and subsequent ageing treatments lead to:

(1) the formation of arrays of extrinsic dis-

locations in all boundaries;

(2) the formation of a matrix dislocation depleted zone adjacent to the boundary;

(3) the creation of "dislocation links" between the matrix and the grain boundary.

5.2.3. Discussion

In the companion paper it was shown that the nucleation of grain boundary precipitates of NbC occurred profusely on extrinsic dislocations [1]. Further, these dislocations might be expected to accelerate both growth and coarsening of grain boundary precipitates for a number of reasons:

(1) rapid diffusion of solute in a grain boundary will occur along extrinsic dislocation lines and, since preferential nucleation occurs on extrinsic dislocations, such particles will automatically be in contact with these diffusion paths;

(2) pipe diffusion of solute along matrix/extrinsic "dislocation links" will increase the rate of solute diffusion towards a grain boundary (adding to any collector plate mechanism operating simultaneously [5]);

(3) additional pipe diffusion links may be generated during ageing when segments of matrix dislocations, which are pinned by particles at the edge of the precipitate depleted zones, climb into the boundary;

(4) extrinsic dislocations will tend to increase the solubility limit of a grain boundary, this increase being a function of the extrinsic dislocation density;

(5) the accumulated strain fields of the extrinsic dislocation content of a boundary will increase its strain energy which, in itself, will lead to an increase in the rate of solute flow towards the grain boundary.

Thus, the increase in mean grain-boundary particle size with increasing levels of deformation is largely a reflection of the increased density of extrinsic dislocations. Similarly, the variations in mean boundary carbide size in the same specimen material will be a function of the relative density of such non-equilibrium defects from boundary to boundary.

The development of precipitate depleted zones and the small mean carbide sizes within these zones is then seen to be controlled by the development of the total grain-boundary microstructure. The depletion of matrix dislocations in this zone will lead to a reduction in the number density of available nucleation sites close to the boundary. Further, as the ageing process continues, both the number density and mean size within the depleted zones will tend to decrease due to the growth/coarsening processes which are occurring at the grain boundary.

6. Conclusions

This paper has demonstrated the quantitative effects of deformation prior to ageing on precipitation in an austenitic stainless steel. Increasing amounts of deformation prior to ageing are seen to decrease the mean matrix precipitate size whilst the mean boundary precipitate size increases. An explanation for this behaviour has been suggested.

This explanation rests on the important role played by extrinsic grain-boundary dislocations which constitute the main non-equilibrium component of grain-boundary structure introduced by deformation. The results of this present investigation suggest that, where large densities of extrinsic dislocations are present, any more subtle effects on the development of grain-boundary precipitate size distributions due to the effects of the underlying equilibrium components of grain-boundary structure, will probably be almost completely suppressed.

Acknowledgements

The authors are grateful to Professor R. W. K. Honeycombe for the provision of laboratory facilities. Financial support from S.R.C. (P.R.H.) and the Springfield Laboratories of U.K.A.E.A. (A.R.J.) is gratefully acknowledged.

References

1. A. R. JONES, P. R. HOWELL and B. RALPH, *J. Mater. Sci.* **11** (1976) 1593.
2. A. R. JONES, Ph.D. Thesis, University of Cambridge (1974).
3. A. R. JONES, P. R. HOWELL, T. F. PAGE and B. RALPH, 4th Bolton Landing Conference on Grain Boundaries in Engineering Materials (1974), edited by J. L. Walter, J. H. Westbrook and D. A. Woodford (A.I.M.E.; A.S.M.; Claitor, 1975), p. 629.
4. D. J. SWINDEN and J. H. WOODHEAD, *J.I.S.I.* **209** (1971) 883.
5. H. I. AARONSON and Y. C. LIU, *Scripta Met.* **2** (1968) 1.

Received 5 February and accepted 9 March 1976.